International Journal of Pharmaceutics 468 (2014) 142–151

Contents lists available at ScienceDirect

International Journal of Pharmaceutics

journal homepage: www.elsevier.com/locate/ijpharm

Pharmaceutical nanotechnology

Preparation, optimization and *in vitro* characterization of stearoyl-gemcitabine polymeric micelles: A comparison with its self-assembled nanoparticles

Zahra Daman [a], SeyedNaser Ostad [b], Mohsen Amini [c], Kambiz Gilani [a,d,*]

[a] Aerosol Research Laboratory, Department of Pharmaceutics, School of Pharmacy, Tehran University of Medical Sciences, Tehran, Iran
[b] Department of Toxicology and Pharmacology, School of Pharmacy, Tehran University of Medical Sciences, Tehran, Iran
[c] Department of Medicinal Chemistry, School of Pharmacy, Tehran University of Medical Science, Tehran, Iran
[d] Medicinal Plants Research Center, Tehran University of Medical Sciences, Tehran, Iran

ARTICLE INFO

Article history:
Received 22 January 2014
Received in revised form 7 April 2014
Accepted 7 April 2014
Available online 13 April 2014

Keywords:
Polymeric micelles
Stearoyl gemcitabine
Poly(ethylene glycol)–poly(D,L-lactide)
Self-assembly
Pancreatic cancer

ABSTRACT

Although gemcitabine (Gem) constitutes first-line therapy for pancreatic cancer, its clinical outcome suffers from rapid metabolism and acquired drug resistance. To overcome its limitations, several lipophilic prodrugs including 4-(*N*)-stearoyl Gem (GemC18) have been studied for their efficacy over Gem. Herein, we aimed to prepare and characterize the GemC18-loaded poly(ethylene glycol)–poly(D,L-lactide) (PEG–PLA) polymeric micelles (PMs) as well as its self-assembled nanoparticles (NPs). A D-optimal design was also utilized to investigate the effects of formulation variables, namely initial drug/polymer ratio, total solid content, and the type of organic solvent on properties of GemC18-loaded PMs. The optimized formulation showed a particle size of about 120 nm, encapsulation efficiency >90%, and a sustained release behavior of the drug. Alternatively, the prodrug NPs were harvested in larger size (~300 nm) and more negative zeta potential, but less chemical stability compared to the optimized PMs. In Panc-1 and AsPC-1 cell lines, both GemC18-loaded PMs and NPs were significantly more cytotoxic than GemC18 solution. Chiefly, they could effectively reduce the viability of Gem high-resistant AsPC-1 cells in culture, whereas the molar equivalent doses of Gem did not show any acceptable cytotoxicity. Thus, these results suggest a promising direction for alternative Gem delivery systems for future therapeutic applications.

© 2014 Elsevier B.V. All rights reserved.

1. Introduction

Pancreatic cancer is one of the leading causes of death from malignant disease with a five-year survival rate of almost 6% from 2001 to 2007, while just a very little improvement has been achieved over this value during the past 30 years (Siegel et al., 2012). Gemcitabine hydrochloride (Gem) is a deoxycytidine analogue, which is the first line treatment for pancreatic cancer (Burris et al., 1997). However, the acquired tumor resistance has become a major problem for Gem-related chemotherapies. This resistance is mainly because of impaired membrane nucleoside transporters, which are responsible for cellular uptake of hydrophilic nucleosides (Oguri et al., 2007). Furthermore, Gem possess a very short half-life and most of its active metabolite is rapidly eliminated from the body with minimal antitumor activity (Immordino et al., 2004). Thus, frequent administration schedules are required which can lead to significant dose-related side effects (Storniolo et al., 1997).

Many efforts have been employed to overcome the shortages associated with this drug. Among them, the prodrug strategy has been widely explored in order to not only overcome the Gem resistance by enhancing its cellular uptake through passive diffusion, but also improve its pharmacokinetic behavior. In this regard, the 4-(*N*)-amino group of Gem is a favorable site for such modifications because the resultant amide derivatives have slower rate of metabolism compared to its ester derivatives on 3′ and 5′ hydroxyl groups (Bender et al., 2009). Several 4-(*N*)-Gem conjugates such as 4-*N*-PEG-Gem (Vandana and Sahoo, 2010), 4-*N*-stearoyl-Gem (GemC18) (Immordino et al., 2004), 4-*N*-squalenoyl-Gem (Couvreur et al., 2006), and 4-*N*-conjugated linoleic acid-Gem (Tao et al., 2012) have been synthesized and shown to have considerable improvements in terms of prolonged

* Corresponding author at: Aerosol Research Laboratory, Department of Pharmaceutics, School of Pharmacy, Tehran University of Medical Sciences, Tehran, Iran. Tel.: +98 21 66959057; fax: +98 21 66461178.
E-mail address: gilani@tums.ac.ir (K. Gilani).

http://dx.doi.org/10.1016/j.ijpharm.2014.04.021
0378-5173/© 2014 Elsevier B.V. All rights reserved.

half-life and *in vivo* antitumor activity. However, their therapeutic efficacy requires a controlled delivery of the lipophilic chemotherapeutic agents to the tumor site. In this regard, nanotechnology-based drug delivery systems can be of great value because of not only their solubility enhancing properties but also the passive and/or active targeting of the anticancer agents directly to the tumor site and reducing the adverse effects.

Therefore, this study was primarily aimed to develop a suitable delivery vehicle for GemC18 derivative. This lipophilic Gem prodrug which had also been described in a patent by Eli Lilly (Myhren et al., 2004), has attracted a good deal of scientific attention during the last years. Several approaches including solid lipid nanoparticles (Sloat et al., 2011), liposomes (Immordino et al., 2004), and PEG-stearic acid micelles (Zhu et al., 2012) have been employed for GemC18 delivery which all showed improved antitumor activity in mice models as compared to Gem alone. In addition, there are data that reveal certain nano-sized GemC18 delivery systems can overcome tumor cells resistance to Gem (Chung et al., 2012).

Among the nanoparticle-based delivery systems, polymeric micelles (PMs) represent promising carriers due to their several advantages including small size (10–200 nm), high stability and solubilizing capacity, sustained drug release, prolonged circulation and accumulation in tumor site (Gong et al., 2012; Nishiyama and Kataoka, 2006). Besides, the use of biodegradable and biocompatible copolymers will ensure the safety of carrier micelles. Poly ethylene glycol (PEG)-b-poly lactic acid (PLA) is a family of FDA-approved copolymers, which possesses excellent micelle forming and drug loading properties and has been extensively studied as a drug delivery vehicle (Kim et al., 2007; Xiao et al., 2010). Thus considering the success of GemC18 in other literature, we hypothesized that its delivery through PEG–PLA PM can share similar advantages. Additionally, we intended to optimize the GemC18-loaded PM by the aid of experimental design in order to determine the main factor effects as well as their possible interactions. This strategy finds the optima with less experimental effort but greater precision than traditional optimization procedures (Leiro et al., 1995).

To our knowledge, the self-assembling properties of GemC18 itself has not being explored in earlier studies. This approach seems interesting, since it was previously shown by Couvreur's group that the amphiphilic 4-*N*-squalenoyl-Gem molecules were able to form spherical self-assemblies of 100–300 nm in water and not only showed slower metabolism, but also displayed more potent anticancer effect on mice with murine metastatic leukemia as compared to Gem (Reddy et al., 2007). As a result, the feasibility of GemC18 self-assembled formulation was also investigated and compared with its PM formulation in terms of physicochemical characteristics, drug release behavior, stability, and *in vitro* cellular uptake and cytotoxicity.

2. Materials and methods

2.1. Materials

Gem base was purchased from Hangzhou Dayangchem Co. Ltd. (Hangzhou, China). mPEG(2k)–PLA(2k) ($M_w/M_n = 1.11$) was supplied from Advanced Polymer Materials Inc. (Montreal, Canada). Stearic acid was from Sigma–Aldrich (Germany).

Triethylamine (TEA), ethylchloroformate, pyrene and 3-(4,5-dimethyl-2-thiazolyl)-2,5-diphenyl-2H-tetrazolium bromide (MTT) were from Merck (Germany). HPLC-grade tetrahydrofuran (THF) and methanol were from Duksan Pure Chemical Co. (Korea). The rest of solvents and chemicals were of analytical grade and supplied locally.

Human pancreatic cancer Panc-1 and AsPC-1 cells were obtained from Pasteur Institute (Tehran, Iran) and grown in RPMI 1640 medium supplemented with 10% fetal bovine serum (FBS), 100 U/mL of penicillin, and 100 μg/mL of streptomycin, all from Biosera (UK).

2.2. Synthesis of 4-(N)-stearoyl-Gem (GemC18)

GemC18 was synthesized according to the previously described method (Immordino et al., 2004). First, 159 mg (0.56 mmol) stearic acid and 56.7 mg (0.56 mmol) TEA were dissolved in 10 mL dry THF, followed by the dropwise addition of 60.8 mg ethylchloroformate (0.56 mmol) under argon atmosphere at −15 °C for 15–20 min to the stirring solution. Then, a solution of Gem (147 mg, 0.56 mmol) in anhydrous dimethylformamide was added and the reaction was carried out at −15 °C with 400 rpm agitation for a few days, as monitored by TLC (dichloromethane/acetone 50:50). The solvent was removed under reduced pressure and the residue was purified by silica gel column chromatography using petroleum ether/ethyl acetate (1:1 v/v) as the eluent to yield 58%. Purity and structure of the GemC18 was confirmed by ^{1}H NMR ($CDCl_3$).

2.3. The critical micelle concentration (CMC) of PEG–PLA

Formation of the PM by the aid of PEG(2k)–PLA(2k) copolymers was studied by fluorescence spectroscopy. Briefly, pyrene (6×10^{-7} M) in acetone was added to series of test tubes and the solvent was evaporated. Then 10 mL of deionized water containing various concentrations of the copolymer from 0.05 to 1000 mg/mL was added to each tube and the solutions were incubated overnight at room temperature under mild stirring. Afterwards, the fluorescent intensity of each sample solution was measured using a spectrofluorometer (Cecil 9000 series, England). To this aim, emission spectra were determined at 372 nm (I_1) and 383 nm (I_3), while the excitation wavelength was fixed at 334 nm. The CMC was determined by taking the midpoint of copolymer concentration at which the relative intensity ratio of I_1/I_3 was varied (Yoo and Park, 2001).

2.4. Preparation of GemC18-loaded PEG–PLA micelles

As the starting point, three different micelle preparation methods (dialysis, thin-film hydration, and solvent evaporation) were used to encapsulate GemC18 within PEG–PLA micelles in order to generate drug-loaded micelles with adequate properties. For all these techniques, an initial drug to polymer (D/P) ratios of 5 and 10% (w/w) were used to prepare the micellar formulations. In the thin-film hydration method, both GemC18 and the polymer were dissolved in THF, followed by vacuum drying and subsequent hydration with deionized water (MilliQ, Millipore) under vigorous stirring in a 70 °C water bath for 30 min. the final concentration of copolymer was fixed at 10 mg/mL. The obtained micelles were then cooled down to room temperature using sonication for 5 min and the micelle-containing supernatant was collected after 10 min centrifugation at 16,000 rpm. The dialysis method consisted of dissolving the drug and the polymer in 4 mL THF, placing within a dialysis bag (M_w cut-off = 8 kDa), and overnight dialyzing against deionized water at room temperature. After dialysis, the micellar solution was centrifuged at 16,000 rpm for 5 min and the supernatant was collected. Finally, the solvent evaporation procedure involved the dissolution of GemC18 and PEG–PLA in THF and dropwise addition of the mixture to MilliQ water under sonication by a Hielscher device (model UP400S, Hielscher ultrasound technology, Germany) with an output power of 50 W for 2 min, followed by the solvent elimination by a rotary vacuum evaporator (Buchi Rotavapor R-124, Buchi, Switzerland). In all cases, the resultant micellar formulations were filtrated through a

0.2 μm Minisart® syringe filter, and immediately investigated in terms of size, zeta potential and loading characteristics.

2.5. Experimental design

Since a high loading efficiency of drugs within the core of PM is an important factor to achieve a maximal therapeutic effect, we chose the solvent evaporation technique for GemC18 micellar formulation preparation based on our preliminary studies (Section 2.4). Upon choosing the best method, it was further optimized in terms of size, polydispersity index (PDI), zeta potential, encapsulation efficiency (EE), and drug loading (DL) by a D-optimal design using Design-Expert® software (version 7.0.0, Stat-Ease, Inc., Minneapolis, MN, USA). However, since the number of experiments increases exponentially with an increasing number of independent variables, some preliminary tests were conducted for several preparation or formulation factors in order to find the most effectual ones and thus keep the number of experiments affordable. These primary independent factors including "the type of organic solvent", "the organic solvent to water ratio (v/v)", "the initial D/P (% w/w)", "total solid content (% w/v)", and "sonication time" were assessed and their levels were determined for the next steps in optimizing procedure. Table 1 shows the main three independent variables and their levels, the generated matrix, and the results of experiments. Data of all dependent variables are the mean of triplicate measurements. The best fitting statistical model to the test data was analyzed by the software and its suitability was evaluated by the "lack of fit" test as well as the plot of the residuals versus predicted values. The significance of the effects of independent variables on the response was assessed by ANOVA and the response surface plots were used to determine the optimum conditions for micelle preparation. Moreover, the predicted data were compared to the experimental values of a freshly prepared batch of the optima in order to demonstrate the suitability of the model.

2.6. Preparation of GemC18 self-assembly

The self-assembled NPs of GemC18 were prepared similarly to its optimized PM formulation. Briefly, 2 mg of the drug was dissolved in 1 mL of THF, and added dropwise to 10 mL of MilliQ water under probe sonication. THF was subsequently removed under reduced pressure using a Rotary evaporator.

2.7. Particle size and zeta potential investigation

Following fabrication, the hydrodynamic diameters, particle size distributions, and zeta potentials of the blank micelles, GemC18-loaded PMs, and GemC18 self-assembled NPs were measured using a dynamic light scattering (DLS) instrument (Zetasizer Nano ZS, Malvern Instruments Ltd., UK). The scattering was observed at 25 °C and 90° angle with respect to the incident beam. The size data were obtained from 16 measurements of 5 s duration and averaged utilizing the instrumental software, while the zeta potentials were acquired based on 100 measurements for each sample.

2.8. Measurement of encapsulation efficiency and drug loading

The filtered GemC18-loaded micellar solutions (5 mL) were centrifuged at 10,000 rpm for 10 min using an ultra filter tube with molecular weight cut-off of 10 kDa (Millipore Co., Bedford, USA) to remove the free drug. The free GemC18 content in the filtrate was measured by a reverse phase chromatographic method using an isocratic HPLC system (Waters, USA) with a UV detector operated at 248 nm and C18 column (5 μm). The mobile phase was methanol and the flow rate was 1 mL/min (Immordino et al., 2004; Sloat et al., 2011). Then, 2 mL THF was added into 1 mL of the same GemC18-loaded micellar solution in order to disrupt the micellar structures. The mixture was bath sonicated (Starsonic60, Liarre, Italy) for 5 min and diluted with methanol before being subjected to HPLC analysis in order to provide the total amount of GemC18 (free and micelle encapsulated). To determine the DL of the formulations, the filtered micellar solutions were lyophilized and the resulting freeze-dried powders were accurately weighed, dissolved in THF, and again analyzed via HPLC to quantify the drug content. The drug loading characteristics were calculated employing the following equations:

$$\mathrm{DL}(\%) = \frac{\text{Drug amount in micelles} - \text{free drug}}{\text{Total micelle amount} - \text{free drug}} \times 100$$

Table 1
Independent and dependent variables, D-optimal design matrix, and results of experimental design.

Run	Independent variables			Dependent variables					
	(*A*)	(*B*)	(*C*)	Y_1	Y_2	Y_3	Y_4	Y_5	Y_6
	D/P ratio[a]	Solid content[b]	Solvent	Prefilter size (nm)	Filtrate size (nm)	PDI	Zeta (mV)	EE (%)	DL (%)
	In range[c]	In range[c]	In range[c]	Minimize[c]	Minimize[c]	Minimize[c]	In range[c]	Maximize[c]	Maximize[c]
1	20	0.4	Acetone	585.2	203.9	0.51	−10.9	20.9	5.7
2	10	0.4	THF	249.7	141.5	0.33	−8.3	79.4	7.3
3	15	0.3	THF	242.3	155.6	0.33	−9.7	68.3	9.8
4	10	0.2	Acetone	363.5	207.3	0.48	−9.8	53.7	4.9
5	15	0.4	Acetone	531.2	198.2	0.53	−8.8	25.8	3.7
6	20	0.2	Acetone	485.1	216.1	0.55	−8.9	24.6	5.6
7	10	0.2	Acetone	370.8	195.5	0.47	−9.4	51.2	4.7
8	20	0.4	THF	306.2	166.4	0.34	−10.4	55.8	12.2
9	10	0.4	Acetone	572.6	190.1	0.51	−9.7	30.9	2.8
10	10	0.4	THF	231.7	150.4	0.27	−11.1	90.7	8.6
11	10	0.2	THF	140.9	128.0	0.21	−12.8	92.6	9.1
12	10	0.4	Acetone	562.1	193.1	0.52	−9.9	34.8	3.1
13	15	0.2	THF	225.2	150.2	0.29	−13.1	85.4	12.1
14	20	0.4	THF	300.8	174.5	0.31	−10.7	52.1	11.8
15	15	0.25	Acetone	496.8	200.1	0.49	−9.5	27.9	3.7
16	20	0.2	THF	266.1	158.0	0.31	−11.5	61.2	12.4
17	20	0.3	Acetone	523.3	204.3	0.55	−11.1	25.5	4.5

[a] Drug to polymer ratio (% w/w).
[b] (% w/v).
[c] Constrain.

$$\text{EE}\,(\%) = \frac{\text{Drug amount in filtered micelles} - \text{free drug}}{\text{Initial drug content in the formulation}} \times 100$$

2.9. TEM investigation

The size and morphology of the GemC18 self-assembled NPs and optimized PMs were examined using a transmission electron microscope (TEM) (Zeiss, EM10C 80 kV, Germany). Briefly, samples were deposited on the carbon-coated copper grids and examined through TEM after being dried at the room temperature.

2.10. Determination of in vitro drug release

The release profile of GemC18 from the optimized PMs and the self-assembled NPs was evaluated using 0.01 M phosphate buffered saline (PBS) containing 0.5% tween80 (pH 7.4) as the dissolution medium. A sample of drug loaded micelles in pure water (2 mL) was introduced into a dialysis membrane bag (M_w cut-off = 8 kDa, Spectrum laboratories, USA), immersed in 26 mL dissolution medium, and incubated at 37 °C under mild stirring rate of 100 rpm. The medium was replaced completely at predefined time points, and the GemC18 concentrations in dissolution medium were determined by the HPLC analysis described previously. All GemC18 release tests were performed in triplicate.

2.11. In vitro stability in 10% FBS

The stability of encapsulated GemC18 in PEG–PLA PMs as well as its self-assembled NPs were investigated by analyzing the drug content after incubation in PBS solution containing 10% (v/v) FBS and maintaining at 37 °C water bath for 24 h. At predefined time intervals (0, 1, 4, 8 and 24 h after incubation), 1 mL of each sample was diluted with 2 mL THF and the mixture was bath sonicated for 5 min, followed by centrifugation at 10,000 rpm for 10 min, and determination of GemC18 content in the supernatant by HPLC. Furthermore, changes in particle sizes of the two aforementioned systems were also recorded once instantly and again after 1 h and 24 h of incubation in 10% FBS at 37 °C.

2.12. In vitro cytotoxicity assay

Panc-1 or AsPC-1 cells were seeded into 96-well plates (10^4 cells/well) and incubated overnight at 37 °C in a humidified atmosphere with 5% CO_2 to allow the cells attach to the plate. Then the culture medium of each well was replaced by 100 μL fresh medium containing serial concentrations (from 1 to 100 μM) of Gem, GemC18 (in less than 1.5% v/v DMSO), GemC18 self-assembled NPs, GemC18-loaded PMs, and blank PEG–PLA micelles (in equivalent concentrations). After 48 h of incubation, the medium was replaced by MTT solution (100 μg/well) and the plates were incubated for additional 4 h, followed by addition of 100 μL DMSO to each well in order to dissolve the formazan crystals. The absorbance was read on a Sunrise absorbance microplate reader (Bio-Rad, Model 680, USA) at dual wavelength of 570 nm. The reported data represented the means of triple measurements. The inhibition of cellular growth relative to control (viability %) was determined at each dose, and the 50% inhibitory concentration (IC_{50}) was calculated for each formulation.

2.13. Cellular uptake assessment

Cellular uptake was studied using Panc-1 and AsPC-1 cell lines. The cells (2×10^5/well) were seeded in 12-well plates and incubated for 24 h at 37 °C and 5% CO_2 to allow the cells to attach. After checking under the microscope for confluency and morphology, the medium was replaced with 1 mL fresh medium containing 40 μg/mL GemC18-containing solution (DMSO < 2% v/v), or self-assembled NP or PM formulation. After 4 h of incubation, the culture medium was removed, cells were washed with cold PBS to terminate the uptake, and lysed with 1% SDS solution in PBS. The cell lysates were diluted with 0.5 mL THF, followed by bath sonication for 5 min to extract all GemC18 content. The supernatant was diluted with methanol and subjected to HPLC after centrifugation at 10,000 rpm for 15 min.

For microscopic analysis, Coumarin-6 (Cou) was chosen as the fluorescent probe for the preparation of Cou-loaded PEG–PLA micelles (copolymer:Cou 400:1 w/w) with the same procedure as that of GemC18-loaded optimized micelles. Afterwards, the seeded AsPC-1 cells were treated by Cou-loaded micelles and maintained at 37 °C for 4 h. the final concentration of Couwas adjusted to 0.5 μg/mL for each well. At last, the cells were washed three times with cold PBS before being examined by a fluorescent microscope (Olympus 1X71, Olympus Biosystems GMBH, Germany).

2.14. Data statistical analysis

All the experiments were carried out at least three times and the results were expressed as the mean ± standard deviation (SD). In addition, all data were compared by ANOVA test. A p-value ≤ 0.05 (two-tail) was considered as statistically significant.

3. Results and discussion

3.1. Synthesis and characterization of GemC18

The well-known mixed-anhydride technique was used to synthesize the lipophilic Gem derivative (GemC18) for micelle encapsulation (Immordino et al., 2004). This method offers a linkage between carboxylic group of a molecule and an amino group of another one. The ^{1}H NMR spectral analysis of the synthesized compound in $CDCl_3$ confirmed the structure assignment:

^{1}H NMR ($CDCl_3$) δ: 10.20 (bs, 1H, NHCO), 8.04 (d, J = 7.5 Hz, 1H, H6), 7.55 (d, J = 7.5 Hz, 1H, H5), 6.30 (*t*, J = 5.2 Hz, 1H, H1′), 5.38–5.45 (*m*, 1H, H3′), 4.41–4.52 (*m*, 1H), 4.23–4.37 (*m*, 1H), 4.14–4.19 (*m*, 1H), 4.05–4.09 (*m*, 1H), 3.86 (dd, J = 8.0 Hz and J = 3.3 Hz, 1H), 2.45–2.50 (*m*, 2H, CO—CH_2), 1.63–1.72 (*m*, 2H, CO—CH_2—CH_2), 1.22–1.35 (*m*, 28H), 0.88 (*t*, J = 7.0 Hz, 3H, CH_3).

3.2. Critical micelle concentration (CMC) of PEG(2k)–PLA(2k)

The CMC value is a crucial factor to determine micelle stability and ease of formation. Herein, the plot of the intensity ratio of the first band (I_1, 372 nm) to the third band (I_3, 383 nm) of pyrene emission spectra as a function of the logarithm of copolymer concentration was used to verify the CMC. Upon micellization in aqueous medium, pyrene molecules partition into the PLA hydrophobic core which dramatically changes the polarity of the pyrene environment and subsequent I_1/I_3 ratio. Fig. 1 indicates that the CMC of PEG(2k)-b-PLA(2k) (*i.e.*, midpoint of copolymer concentration at which the I_1/I_3 substantially decreases) was 3.16 μg/mL which is in accordance with other literature values in water (Lee et al., 2007).

3.3. Effect of different micelle fabrication methods on drug encapsulation

The objective of this study was to develop a polymeric micellar formulation that can effectively encapsulate GemC18 with adequate DL and minimal loss of the drug. Thus, three different methods were investigated for GemC18-loaded micelle generation.

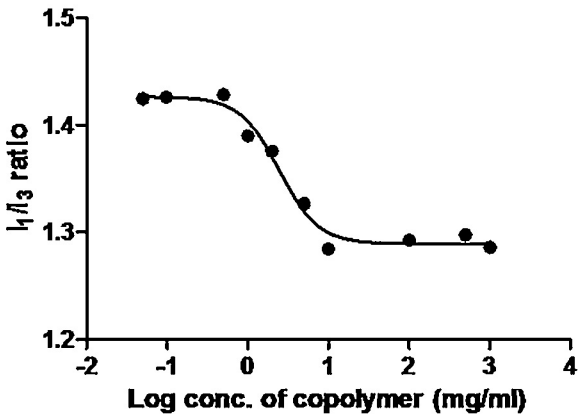

Fig. 1. Plot of I_1/I_3 values versus the log concentration of PEG(2k)–PLA(2k) in water.

As shown in Table 2, the film hydration method produced micelles with the lowest DL (0.41%) and EE (4.52%) at 10% theoretical loading. However, addition of a lipid additive namely tocopheryl polyethylene glycol succinate (TPGS) during micelle formation by this method, markedly contributed to drug solubility through enhancing the hydrophobic interactions between the drug and its chains (Mu et al., 2005). Indeed, it improved the GemC18 loading into PEG–PLA micelles to a loading percentage of nearly 2%, and EE of approximately 20% (data not shown). On the other hand, the dialysis procedure did not provide any significant enhancement in DL properties over the previous method. Since the increase in drug dissolution within the polymer matrix correlates with increase in DL (Panyam et al., 2004), it seems that the two above mentioned methods were not able to prevail the drug–drug interactions and hence, molecularly solubilize GemC18 within the polymer matrix.

Conversely, the solvent evaporation method produced the highest GemC18 loading into PM among all preparation methods, with 9.07% DL at an initial D/P ratio of 10%, and EE of 92.36%. So putting all together, these data convinced us to use the latter procedure for effective loading of GemC18 into PEG–PLA micelles in order to be more investigated as a micellar anticancer system. In fact, this technique is a widely-used method for micelle formation, and has been shown in an earlier study by Nasongkla et al. that can lead to high doxorubicin loading into PEG–PLA micelles (Nasongkla et al., 2006).

Finally, the blank PMs and GemC18 self-assembled NPs were prepared by the same solvent evaporation method and were characterized in terms of size and zeta potential. As seen in Table 2, the drug self-assembly led to noticeably larger particles with the *z*-average diameter of about 340 nm and a higher negative zeta potential of −35.8 mV compared to its PM formulation.

3.4. Experimental design

An optimization process based on a D-optimal design was applied for the preparation of GemC18-loaded micelles. This design minimizes the uncertainty of the model coefficients and is built algorithmically to provide the most precise estimates of the model equations (Lee and Huang, 2011). Before designing the experimental conditions, some preliminary studies were performed in order to identify the most critical independent variables.

3.4.1. D-optimal design and analysis

In the present study, three independent variables including the initial D/P ratio (A), the total solid content (B), and the type of organic solvent (C), along with six responses consisting of nanomicelles particle size before filtering (Y_1) and after filtering (Y_2), polydispersity index (PDI) (Y_3), zeta potential (Y_4), EE (Y_5), and DL (Y_6) were selected for optimization studies (Table 1). Table 3 shows the analysis of variance for the models and terms. For all the suggested models, the lack of fit tests demonstrated that it was not significant relative to the pure error. In addition, the normal probability plots of all fitted models exhibited similarity to straight line and were indicative of normally distributed residuals (data not shown).

GemC18-loaded nanomicelles were produced in the sizes varied between 140.9 ± 3.5 and 585.1 ± 7.9 nm before being subjected to syringe filtering. Regarding statistical analysis performed by the software, it was observed that a 2FI Model was significantly fitted on data obtained for particle size measurements at this stage and all the main numerical factors had significant positive effect on particle size and the type of solvent showed the strongest impact. However, since the interaction of AC was not statistically significant, we excluded this term from the equation:

$$\text{Modified } Y_1 = +370.47 + 39.69A + 49.28B + 129.08C - 20.24AB + 18.68BCR^2 = 0.9867$$

Previous research had shown that the solvent used for drug incorporation into PM can have substantial effects on micelle properties including particle diameter (Harada et al., 2011). When we used THF as the solvent, we obtained much smaller micelles compared to the micelles prepared by the aid of acetone. It is possible that the higher GemC18 solubility in THF is responsible for smaller micelle diameters through inhibiting the large aggregates' formation of GemC18 molecules.

The next parameter that led to size enlargement was the total solid content. Actually, It is supposed that by increasing the number of polymer chains per volume unit of the solvent, it becomes more difficult for the solvent to diffuse into aqueous phase during vacuum evaporation, and thus formation of larger micelles can be expected (Lamprecht et al., 2000). In addition, the

Table 2
GemC18-loaded micelle properties from different fabrication methods (data expressed as mean ± SD).

Fabrication method	Theoretical loading (%)	Micelle size (nm)	Zeta potential (mV)	Encapsulation efficiency (%)	Drug loading (%)
Film hydration	5	26.75 ± 1.3	−5.45 ± 0.6	7.21 ± 0.9	0.31 ± 0.08
	10	37.16 ± 2.8	−4.97 ± 0.8	4.52 ± 1.2	0.41 ± 0.1
Dialysis	5	22.86 ± 2.5	−8.15 ± 1.1	8.29 ± 1.6	0.37 ± 0.05
	10	22.44 ± 1.8	−8.25 ± 0.9	21.52 ± 0.8	1.95 ± 0.2
Solvent evaporation	5	106.14 ± 5.6	−11.7 ± 2.0	94.13 ± 1.7	4.32 ± 0.6
	10	120.71 ± 9.1	−12.8 ± 1.3	92.36 ± 2.2	9.07 ± 0.5
	Blank micelles	41.67 ± 3.4	−3.31 ± 0.5	–	–
	GemC18 self-assembly	339.91 ± 15.2	−35.8 ± 2.4	–	–

Table 3
A summary of fitted model analysis for responses Y_1 (prefiltration particle size, nm), Y_2 (filtrate particle size, nm), Y_3 (PDI), Y_5 (EE %) and Y_6 (DL %).

Response		Model	Terms							R^2
			Intercept	*A*	*B*	*C*	*AB*	*AC*	*BC*	
Y_1	Coefficient	–	+370.04	+40.54	+49.08	+128.66	−21.89	−8.67	+18.47	0.9894
	p-value	<0.0001	–	<0.0001	<0.0001	<0.0001	0.003	0.14	0.005	–
Y_2	Coefficient	–	+176.90	+9.60	+0.63	+24.79	−0.94	−3.80	−5.57	0.9795
	p-value	<0.0001		<0.0001	0.6435	<0.0001	0.541	0.021	0.0018	
Y_3	Coefficient	–	+0.41	+0.023	0.015	0.11	–	–	–	0.9551
	p-value	<0.0001	–	0.0103	0.0605	<0.0001	–	–	–	
Y_5	Coefficient	–	+52.83	−12.42	−5.76	−21.08	–	–	–	0.9550
	p-value	<0.0001	–	<0.0001	0.0026	<0.0001	–	–	–	
Y_6	Coefficient	–	+7.44	+1.23	−0.52	−3.04	+0.34	−0.56	+0.074	0.9742
	p-value	<0.0001	–	0.0001	0.0205	<0.0001	0.141	0.019	0.705	

particle size wasenlarged by increasing the initial D/P ratio, which might be caused by increasing GemC18 content in the core of micelles.

Since the filteration (0.2 μm pore size) is a crucial step in nanoparticle formation and sterilization prior to cellular studies, we included this technique in our micelle formation process. Based on statistical analysis of the size data measured after filtering the nanomicellar solutions (Y_2), a notably fitted 2FI model ($p < 0.0001$) was obtained by using the Design-Expert software. Similar to the primary size measurment, the solvent type had the most powerful effect on the filterate size followed by the initial D/P ratio and the interactions of *AC* and *BC*. Upon excluding the insignificant terms of *B* and *AB*, the equation was changed into the following one, while a three-dimensional response surface plot based on this equation is presented in Fig. 2a.

$$\text{Modified } Y_2 = +176.89 + 9.44A + 0.76B + 24.78C - 3.64AC$$
$$-5.44BCR^2 = 0.9787$$

According to statistical analysis of the PDI measurements (Y_3), a linear model was significantly fitted on these data. However, the effect of the solid content on PDI was not significant ($p > 0.05$), and thus, it could be excluded from the main equation without changing the other coefficients.

Regarding the zeta potential, it should be mentioned that small amplitude differences were found between the responses, indicating a minor influence of the formulation variables on the surface properties of nanomicelles. The zeta potential values showed an overall negative mean value of −10.34 mV.

It is obvious that a high loading characteristics of any colloidal carrier system is of great importance in order to diminish the total amount of delivery system intended to be used as the dosage unit. As presented in Table 1 the EE of the filtered nanomicellar solutions showed a wide variation from 20.9% (run 1) to 92.6% (run 11) indicating that this response was strongly dependent on the chosen variables. The results showed that the EE rapidly increased as THF was used during the preparation of PMs. However, increasing the D/P ratio as well as the solid content led to noticeable reduction in EE mainly because of corresponding elevation of nanomicelles' size which promotes the removal of larger drug-loaded micelles during the filteration (Fig. 2b). Also, according to the results obtained from DL measurments, the value of DL% varied from 2.8% to 12.1% and was positively influenced by all the three variables including the intial D/P ratio which is consistent with the findings of other literature (Wang et al., 2007; Wei et al., 2009). Fig. 3a is a graphical representation of the effects of D/P ratio and the total solid content on the DL reponse while THF was applied as the solvent.

It is worth mentioning that even at the lowest DL (%), the water solubility of this Gem prodrug was successfully increased compared to its intrinsic limit. For instance, at the loading level of 2.8% in formulation 9, the concentration of GemC18 was 56 μg/mL, which was 5 times higher than its measured solubility of about 10 μg/mL.

3.4.2. Multi-objective optimization and characteristics

In this study, the desirability function (Deming, 1991) was calculated by the Design-Expert software based on the criteria for simultaneously attaining the minimum of nanomicelles size (before and after filtration Y_1, Y_2) and PDI (Y_3), while maximizing EE (Y_5) and the DL (Y_6). The zeta potential (Y_4) was assigned in

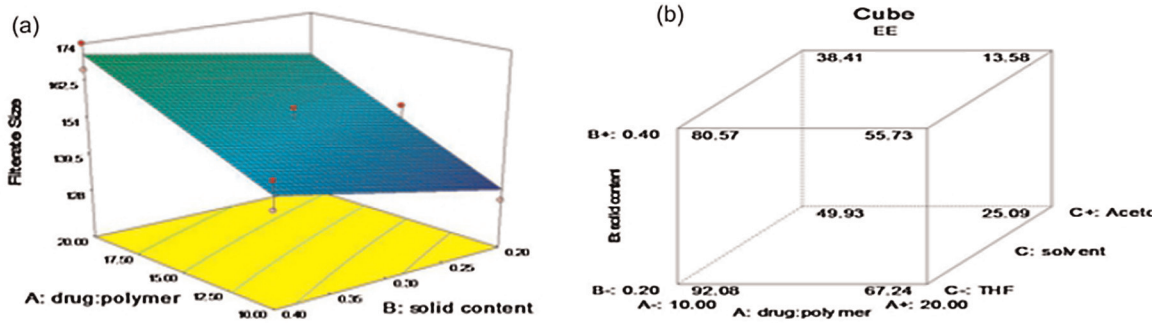

Fig. 2. (a) Response surface plot showing the effects of (*A*) and (*B*) on response (Y_2), while using THF as the solvent (*C*), (b) cube plot showing the effects of variables (*A*), (*B*), and (*C*) on response (Y_5).

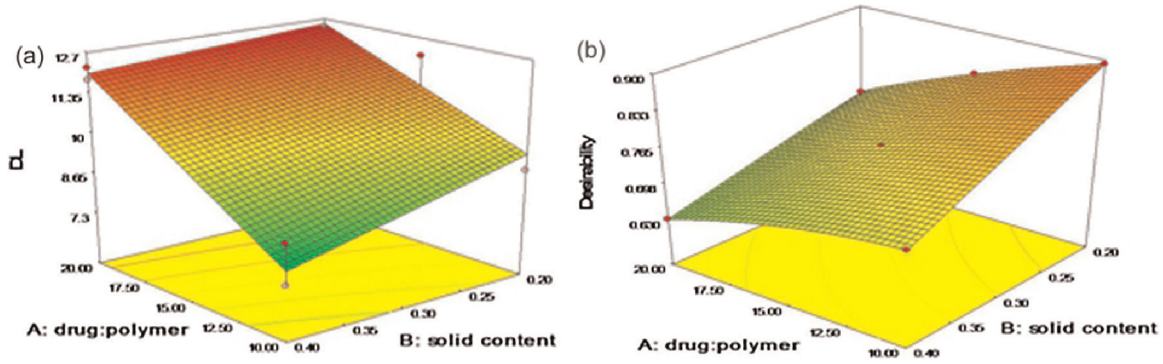

Fig. 3. (a) Response surface plot showing the effects of (*A*) and (*B*) on response (Y_6), while using THF as the solvent (*C*), (b) the relation between overall desirability and variables (*A*) and (*B*).

Table 4
The observed versus predicted response values for the optimized formulation.

Independent variable	Optimized level		
A: initial drug/polymer (% w/w)	10		
B: total solid content (% w/v)	0.2		
C: solvent	THF		
Overall desirability	0.901		
Dependent variable	**Expected**	**Observed**	**Residual**
Y_1 : prefiltration particle size (nm)	150.844	139.91	−10.934
Y_2 : filtrate particle size (nm)	131.579	128.73	−2.849
Y_3 : PDI	0.2594	0.2311	−0.0283
Y_4 : zeta potential (mV)	−12.773	−10.85	1.923
Y_5 : encapsulation efficiency (%)	92.0828	93.28	1.197
Y_6 : drug loading (%)	9.64432	9.325	−0.319

range. The desirability (*D*) varies between *D* = 0 for fully undesired response and *D* = 1 for completely desired one. Fig. 3b describes the relationship between the overall desirability and AB variables. It indicates that the highest value of *D* (0.9) could be obtained by applying the initial D/P ratio of 10% (w/w), total solid content of 0.2% (w/v) and THF as the organic solvent. Finally, a new batch of the optimized formulation with the predicted levels of independent variables was prepared and evaluated in triplicate in order to confirm the validity and precision of the model. The observed and predicted values are presented in Table 4. The reasonable agreement between the two corresponding values indicated that the model equations adequately described the influences of selected factors on the characteristics of PEG–PLA nanomicelles.

The TEM image of the optimized formulation is shown in Fig. 4a. The GemC18-loaded PM exhibited spherical morphology and the particle size of about 120 nm, which was in good agreement by the results obtained through DLS technique. This dimension can be desirable since the particles with the size of less than 200 nm are less susceptible to reticuloendothelial uptake (Gaucher et al., 2005). By close investigation of the TEM images, it was observed that the core of micelles were slightly darker than their shell. These dark regions should be attributed to PLA block of the copolymer as well as the stearic acid chains of the entrapped drug molecules and the bright regions should respond to the hydrophilic PEG. This kind of core–shell structure of PEG–PLA micelles plays an important role in providing long circulation times in blood because the hydrophilic PEG corona on the micelles surface creates a barrier layer to prevent the recognition of the micelles by phagocytic cells which subsequently reduces their accumulation in the reticuloendothelial system (RES) (Owens and Peppas, 2006). Interestingly, this kind of structure was also visible in the TEM image of GemC18 self-assembled NP in Fig. 4b, which represents a hydrophilic Gem corona along with a hydrophobic lipid core. However, these spherical NPs showed a larger size, denser core and more regular edges than the corresponding PM.

In vitro GemC18 release from PEG–PLA micelles was investigated by dialysis method using PBS (pH 7.4) containing 0.5% (w/w) tween80 as the release medium, which provided the sink condition required for this experiment. As seen in Fig. 5, the release of GemC18 from the PM was noticeably slowed down since only 30% of GemC18 was released from the micelles in 72 h. Regarding the drug release from its self-assembled NPs, we found it in a more retarded manner than the optimized PM. These results demonstrates the stability of both the nano formulations which may be attributed to the high affinity between the stearic acid domains of the drug molecules themselves as well as the hydrophobic core of PMs.

Finally, an important aspect for *in vivo* applications concerns the stability of drug-loaded nanomicelles in the biological medium. Fig. 6a represents the percentage of GemC18 remaining

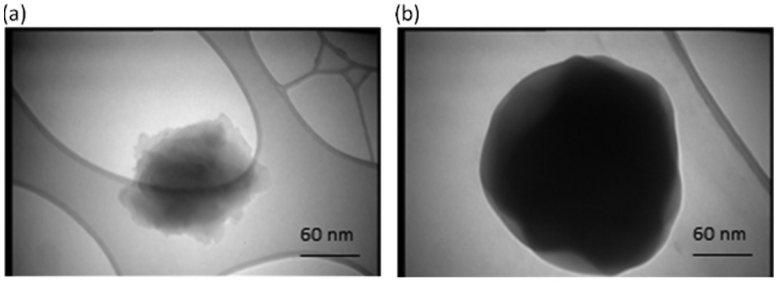

Fig. 4. TEM images of (a) GemC18-loaded polymeric micelles; (b) GemC18 self-assembled nanoparticles.

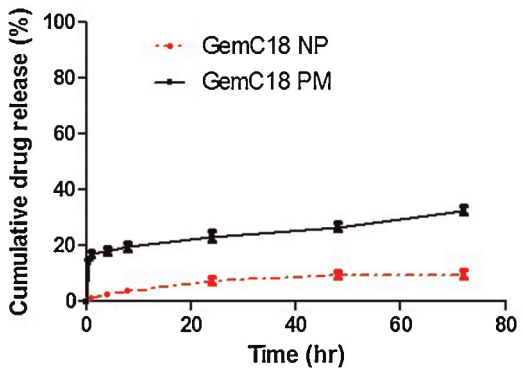

Fig. 5. *In vitro* release of GemC18 from polymeric micelles and its self-assembled nanoparticles.

in micelles in comparison with its self-assembled NPs after 24 h of incubation with PBS containing 10% (v/v) FBS at 37 °C. This study showed that almost 80% of the GemC18 remained in the micelles after 24 h incubation with FBS, while this amount decreased to about 63% for GemC18 self-assemblies after the same period of incubation in similar conditions. Furthermore, the changes in particle size of GemC18 optimized PMs and its self-assembled NPs were evaluated in order to investigate the physical stability of the formulations. As seen in Fig. 6b, the size of both the GemC18-containing nano formulations slightly decreased ($p < 0.05$) after 1 h of incubation in 10% FBS. However, a noticeable decrease ($p < 0.05$) in particle size was clear after the overnight incubation which can be due to hydrolysis of the drug and/or the copolymer and subsequent reduction in the content of the nano formulations. In summary, these data suggest that the GemC18 micelle formulation may act more favorably than its self-assemblies for future *in vivo* applications since the PEG shielding and subsequent high physicochemical stability are important factors in determining the circulation behavior of a drug delivery system.

3.5. Evaluation of in vitro cytotoxicity and cellular uptake

As shown in Fig. 7a, the prodrug GemC18 solution indicated less cytotoxicity than the parent drug (IC_{50} of 29.24 μM) in Panc-1 cells with an almost two folds greater IC_{50} value. However, formulating the GemC18 molecules into self-assembled NPs as well as PEG–PLA PMs noticeably decreased the IC_{50} values to 19.49 and 25.64 μM, respectively. Despite possessing higher IC_{50}, the polymeric micellar formulation showed greater growth inhibitory activity than the nano self-assemblies at high drug concentrations. This observation could have been caused by a possible carrier-mediated synergistic effect. Actually, the blank micelles showed no significant toxicity in low concentrations, but about 20% decrease in Panc-1 viability was observed at high polymer concentrations equivalent to 100 μM GemC18 (data not shown).

The cytotoxic activity of formulations was additionally assayed on highly metastatic AsPC-1 cell line (Fig. 7b). Interestingly, while the free Gem solution did not elicit at least 50% cell death even at high drug concentrations, its prodrug nano formulations considerably improved the cytotoxicity and overcame its high resistance.

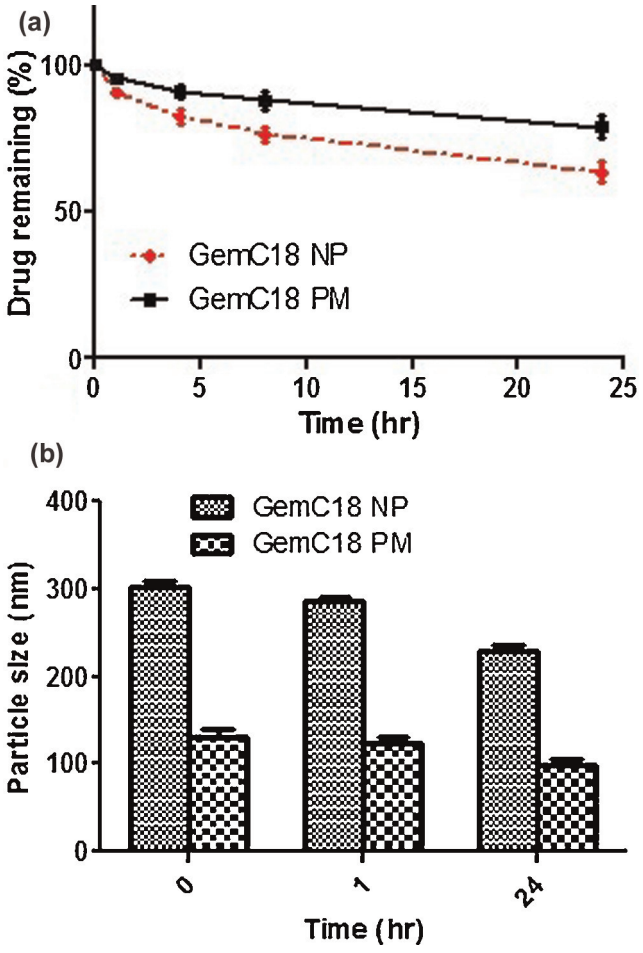

Fig. 6. *In vitro* stability of GemC18-loaded polymeric micelles and its self-assembled nanoparticles. (a) Percentage of GemC18 remained and (b) particle sizes after incubation in 10% FBS at 37 °C.

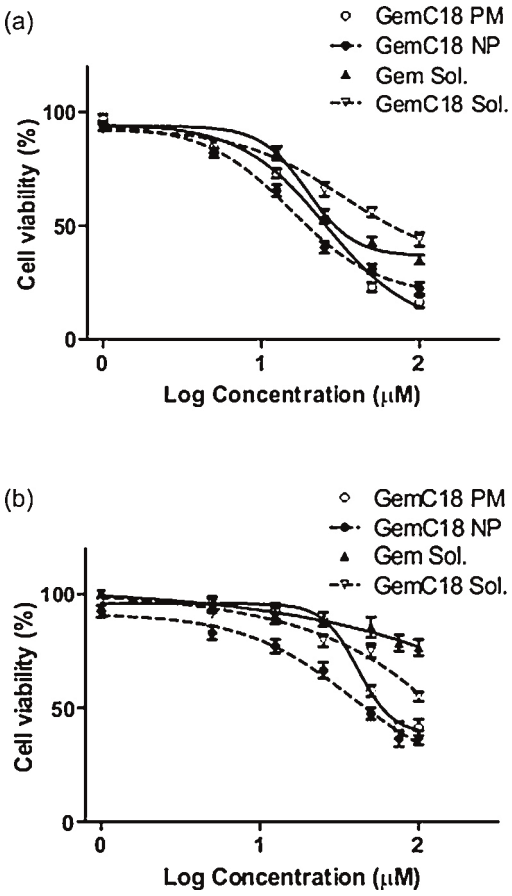

Fig. 7. Cytotoxicity of the formulations on human pancreatic cancer cells: (a) Panc-1 cell line, (b) AsPC-1 cell line.

This observation can be of great value since the acquired resistance is the major problem associated with Gem-based chemotherapies. The resistance of AsPC-1 cells to Gem had been previously confirmed by linking it to different mechanisms such as the epithelial–mesenchymal transition (EMT) program in resistant cancerous cells (Arumugam et al., 2009). In accordance with our results, certain GemC18 NPs were shown to be able to overcome tumor cells resistance to Gem (Chung et al., 2012). The results also revealed that GemC18 PMs (IC_{50} = 58.88 μM) and self-assembled NPs (IC_{50} = 46.34 μM) had stronger inhibitory effects than GemC18 solution. Similar to Panc-1 cells, the blank PEG–PLA micelles showed no significant toxicity on these cells, while just a ~10% cell death was observed at the maximum polymer concentration used for embedding 100 μM GemC18.

Cellular uptake of GemC18 solution as well as its self-assembled NP and PM formulation was studied both qualitatively and quantitatively, by the aid of fluorescence microscopy and direct determining the GemC18 concentration in the cells, respectively. Fig. 8a shows the cellular uptake percentage of the mentioned formulations in Panc-1 and AsPC-1 cell lines after 4 h of incubation at 37 °C. It was found that in AsPC-1 cells, GemC18 self-assembled NPs were more efficiently taken up (29.75 ± 2.61%) than the optimized PM and GemC18 solution with 15.95 ± 2.05% and 20.35 ± 1.62% of drug uptake, respectively ($p < 0.05$). Similar trend could be observed in Panc-1 cells, wherein the percentage of internalized drug was 37.55 ± 2.21% for GemC18 NP, 28.60 ± 1.85% for GemC18 PM, and 30.11 ± 1.98% for GemC18 solution. So the enhanced cytotoxicity of GemC18 self-assemblies in both cells-could be attributed to the improved cellular uptake of the drug. On the other hand, we expected that its higher negative zeta potential might have retarding effect on its cellular uptake. Thus, there might be other mechanisms for the cellular internalization of GemC18 self-assembled NP such as diffusive uptake and/or accumulation in cellular membrane rather than endocytosis-mediated pathway. In this regard, Bildstein et al. had reported the probable aforementioned uptake mechanism for squalenoyl-Gem nano self-assemblies, which structurally resembles our GemC18 self-assembled NP (Bildstein et al., 2010).

It was also found that the uptake of GemC18 solution was not statistically different ($p > 0.05$) from that of encapsulated in PM in both cell lines, but its antiproliferative activity was inferior to those of nano-formulations. As mentioned before, a high uptake of lipophilic drugs is possible as they can easily cross the cell membranes (Li et al., 2010). However, the weaker effect of GemC18 solution is likely to be due to its low hydrolytic metabolism as compared to its nano micelles and self-assemblies. Indeed, the amide bonds are relatively stable in physiological and slightly acidic conditions. Thus, it seems that the passively diffused prodrug solution into the whole cytoplasm could not be metabolized as fast as its nano micelle formulation which is likely to be subjected to the more efficient lysosomal enzymatic degradation upon its endosomal internalization (Zhu et al., 2012).

Fig. 8b shows a qualitative fluorescent microscopic image of AsPC-1 cells after 4 h incubation with Cou-loaded PM at 37 °C. The fluorescent intensity in the cell cytoplasm demonstrates the ability of PEG–PLA micelles to be well taken up by these cells.

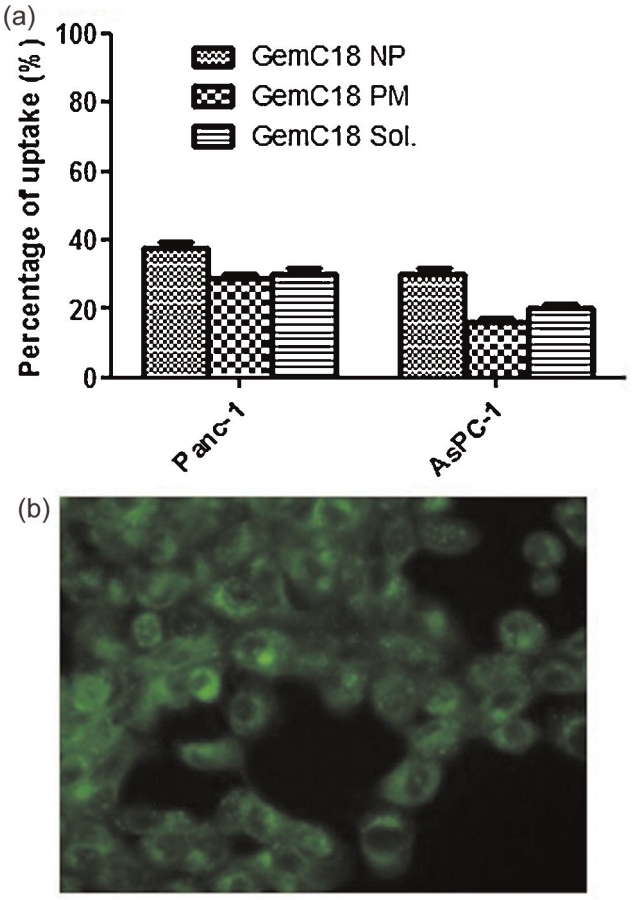

Fig. 8. (a) Percentage of GemC18 internalized by human pancreatic cancer cells after 4 h incubation at 37 °C, (b) fluorescent microscopy image of ASPC-1 cells incubated with coumarin-loaded PEG–PLA micelles for 4 h at 37 °C.

4. Conclusion

In the present study, we reported new nanoparticle-based Gem prodrug formulations that showed promising *in vitro* anticancer activity. In this regard, GemC18-loaded optimized PEG–PLA PMs as well as the drug's self-assembled NPs were prepared and investigated in terms of physicochemical characteristics, drug release behavior and *in vitro* cytotoxicity effects. Chiefly, both of the formulations showed enhanced *in vitro* cytotoxicity compared to Gem and GemC18 solutions on pancreatic cancer cell lines suggesting that they can be effective Gem delivery systems for future clinical applications. Additionally, the drug's self-assembled NPs showed superior *in vitro* cellular uptake and cytotoxicity than its PM formulation. However, it possessed less chemical stability in 10% FBS compared to the polymeric system. Of course, further *in vivo* anticancer activity studies should be performed in order to better compare these GemC18 delivery systems with each other as well as the conventional Gem solution. Aside from stability issues, another possible advantage of PM formulation for *in vivo* applications may be the feasibility of active drug targeting to the tumor site, which is the topic of our future project.

Acknowledgment

This research has been supported by Tehran University of Medical Sciences & Health Services (grant number 91-03-33-19300).

References

Arumugam, T., Ramachandran, V., Fournier, K.F., Wang, H., Marquis, L., Abbruzzese, J. L., Gallick, G.E., Logsdon, C.D., Conkey, Mc, Choi, D.J., W, 2009. Epithelial to mesenchymal transition contributes to drug resistance in pancreatic cancer. Cancer Research 69, 5820–5828.

Bender, D.M., Bao, J., Dantzig, A.H., Diseroad, W.D., Law, K.L., Magnus, N.A., Peterson, J.A., Perkins, E.J., Pu, Y.J., Reutzel-Edens, S.M., 2009. Synthesis, crystallization, and biological evaluation of an orally active prodrug of gemcitabine. Journal of Medicinal Chemistry 52, 6958–6961.

Bildstein, L., Dubernet, C., Marsaud, V., Chacun, H., Nicolas, V., Gueutin, C., Sarasin, A., Benech, H., Lepetre-Mouelhi, S., Desmaele, D., 2010. Transmembrane

diffusion of gemcitabine by a nanoparticulate squalenoyl prodrug: an original drug delivery pathway. Journal of Controlled Release 147, 163–170.
Burris, H.r., Moore, M.J., Andersen, J., Green, M.R., Rothenberg, M.L., Modiano, M.R., Cripps, M.C., Portenoy, R.K., Storniolo, A.M., Tarassoff, P., 1997. Improvements in survival and clinical benefit with gemcitabine as first-line therapy for patients with advanced pancreas cancer: a randomized trial. Journal of Clinical Oncology 15, 2403–2413.
Chung, W.-G., Sandoval, M.A., Sloat, B.R., Lansakara-P, D.S., Cui, Z., 2012. Stearoyl gemcitabine nanoparticles overcome resistance related to the over-expression of ribonucleotide reductase subunit M1. Journal of Controlled Release 157, 132–140.
Couvreur, P., Stella, B., Reddy, L.H., Hillaireau, H., Dubernet, C., Desmaële, D., Lepêtre-Mouelhi, S., Rocco, F., Dereuddre-Bosquet, N., Clayette, P., 2006. Squalenoyl nanomedicines as potential therapeutics. Nano Letters 6, 2544–2548.
Deming, S.N., 1991. Multiple-criteria optimization. Journal of Chromatography A 550, 15–25.
Gaucher, G., Dufresne, M.-H., Sant, V.P., Kang, N., Maysinger, D., Leroux, J.-C., 2005. Block copolymer micelles: preparation, characterization and application in drug delivery. Journal of Controlled Release 109, 169–188.
Gong, J., Chen, M., Zheng, Y., Wang, S., Wang, Y., 2012. Polymeric micelles drug delivery system in oncology. Journal of Controlled Release 159, 312–323.
Harada, Y., Yamamoto, T., Sakai, M., Saiki, T., Kawano, K., Maitani, Y., Yokoyama, M., 2011. Effects of organic solvents on drug incorporation into polymeric carriers and morphological analyses of drug-incorporated polymeric micelles. International Journal of Pharmaceutics 404, 271–280.
Immordino, M.L., Brusa, P., Rocco, F., Arpicco, S., Ceruti, M., Cattel, L., 2004. Preparation, characterization, cytotoxicity and pharmacokinetics of liposomes containing lipophilic gemcitabine prodrugs. Journal of Controlled Release 100, 331–346.
Kim, D.-W., Kim, S.-Y., Kim, H.-K., Kim, S.-W., Shin, S., Kim, J., Park, K., Lee, M., Heo, D., 2007. Multicenter phase II trial of genexol-PM, a novel cremophor-free, polymeric micelle formulation of paclitaxel, with cisplatin in patients with advanced non-small-cell lung cancer. Annals of Oncology 18, 2009–2014.
Lamprecht, A., Ubrich, N., Hombreiro Perez, M., Lehr, C.-M., Hoffman, M., Maincent, P., 2000. Influences of process parameters on nanoparticle preparation performed by a double emulsion pressure homogenization technique. International Journal of Pharmaceutics 196, 177–182.
Lee, C.-P., Huang, M.-N.L., 2011. D-optimal designs for second-order response surface models with qualitative factors. Journal of Data Science 9, 139–153.
Lee, S.C., Huh, K.M., Lee, J., Cho, Y.W., Galinsky, R.E., Park, K., 2007. Hydrotropic polymeric micelles for enhanced paclitaxel solubility: in vitro and in vivo characterization. Biomacromolecules 8, 202–208.
Leiro, J., Siso, M., Ortega, M., Santamarina, M., Sanmartin, M., 1995. A factorial experimental design for investigation of the effects of temperature, incubation time, and pathogen-to-phagocyte ratio on *in vitro* phagocytosis by turbot adherent cells. Comparative Biochemistry and Physiology Part C: Pharmacology, Toxicology and Endocrinology 112, 215–220.
Li, Q., Du, Y.-Z., Yuan, H., Zhang, X.-G., Miao, J., Cui, F.-D., Hu, F.-Q., 2010. Synthesis of lamivudine stearate and antiviral activity of stearic acid-g-chitosan oligosaccharide polymeric micelles delivery system. European Journal of Pharmaceutical Sciences 41, 498–507.
Mu, L., Elbayoumi, T., Torchilin, V., 2005. Mixed micelles made of poly(ethylene glycol)-phosphatidylethanolamine conjugate and d-α-tocopheryl polyethylene glycol 1000 succinate as pharmaceutical nanocarriers for camptothecin. International Journal of Pharmaceutics 306, 142–149.
Myhren F., Borretzen B., Dalen A., Sandvold M.L., 2004. Gemcitabine derivatives. EP Patent 0,986,570.
Nasongkla, N., Bey, E., Ren, J., Ai, H., Khemtong, C., Guthi, J.S., Chin, S.-F., Sherry, A.D., Boothman, D.A., Gao, J., 2006. Multifunctional polymeric micelles as cancer-targeted, MRI-ultrasensitive drug delivery systems. Nano Letters 6, 2427–2430.
Nishiyama, N., Kataoka, K., 2006. Current state, achievements, and future prospects of polymeric micelles as nanocarriers for drug and gene delivery. Pharmacology & Therapeutics 112, 630–648.
Oguri, T., Achiwa, H., Muramatsu, H., Ozasa, H., Sato, S., Shimizu, S., Yamazaki, H., Eimoto, T., Ueda, R., 2007. The absence of human equilibrative nucleoside transporter 1 expression predicts nonresponse to gemcitabine-containing chemotherapy in non-small cell lung cancer. Cancer Letters 256, 112–119.
Owens III, D.E., Peppas, N.A., 2006. Opsonization, biodistribution, and pharmacokinetics of polymeric nanoparticles. International Journal of Pharmaceutics 307, 93–102.
Panyam, J., Williams, D., Dash, A., Leslie-Pelecky, D., Labhasetwar, V., 2004. Solid-state solubility influences encapsulation and release of hydrophobic drugs from PLGA/PLA nanoparticles. Journal of Pharmaceutical Sciences 93, 1804–1814.
Reddy, L.H., Dubernet, C., Mouelhi, S.L., Marque, P.E., Desmaele, D., Couvreur, P., 2007. A new nanomedicine of gemcitabine displays enhanced anticancer activity in sensitive and resistant leukemia types. Journal of Controlled Release 124, 20–27.
Siegel, R., Naishadham, D., Jemal, A., 2012. Cancer statistics. CA: A Cancer Journal for Clinicians 62, 10–29.
Sloat, B.R., Sandoval, M.A., Li, D., Chung, W.-G., Lansakara-P, D.S., Proteau, P.J., Kiguchi, K., Giovanni, Di, Cui, J., Z, 2011. *In vitro* and *in vivo* anti-tumor activities of a gemcitabine derivative carried by nanoparticles. International Journal of Pharmaceutics 409, 278–288.
Storniolo, A.M., Allerheiligen, S.R., Pearce, H.L., 1997. Preclinical, pharmacologic, and phase I studies of gemcitabine. Seminars in Oncology 24, S7-2–S7-7.
Tao, X.-M., J, -c., J, -b., Feng, Q., S, -y., Zhang, L.-R., Zhang, Q., 2012. Enhanced anticancer activity of gemcitabine coupling with conjugated linoleic acid against human breast cancer *in vitro* and *in vivo*. European Journal of Pharmaceutics and Biopharmaceutics 82, 401–409.
Vandana, M., Sahoo, S.K., 2010. Long circulation and cytotoxicity of PEGylated gemcitabine and its potential for the treatment of pancreatic cancer. Biomaterials 31, 9340–9356.
Wang, Y., Yu, L., Han, L., Sha, X., Fang, X., 2007. Difunctional pluronic copolymer micelles for paclitaxel delivery: synergistic effect of folate-mediated targeting and pluronic-mediated overcoming multidrug resistance in tumor cell lines. International Journal of Pharmaceutics 337, 63–73.
Wei, Z., Hao, J., Yuan, S., Li, Y., Juan, W., Sha, X., Fang, X., 2009. Paclitaxel-loaded pluronic P123/F127 mixed polymeric micelles: formulation, optimization and in vitro characterization. International Journal of Pharmaceutics 376, 176–185.
Xiao, R.Z., Zeng, Z.W., Zhou, G.L., Wang, J.J., Li, F.Z., Wang, A.M., 2010. Recent advances in PEG–PLA block copolymer nanoparticles. International Journal of Nanomedicine 5, 1057.
Yoo, H.S., Park, T.G., 2001. Biodegradable polymeric micelles composed of doxorubicin conjugated PLGA–PEG block copolymer. Journal of Controlled Release 70, 63–70.
Zhu, S., Lansakara-P, D.S., Li, X., Cui, Z., 2012. Lysosomal delivery of a lipophilic gemcitabine prodrug using novel acid-sensitive micelles improved its antitumor activity. Bioconjugate Chemistry 23, 966–980.